



Cite this: *Chem. Commun.*, 2017, 53, 10520

Received 31st July 2017,  
Accepted 30th August 2017

DOI: 10.1039/c7cc05971j

rsc.li/chemcomm

## Rational design of a fast and selective near-infrared fluorescent probe for targeted monitoring of endogenous nitric oxide†

Junma Tang, Zhiqian Guo,  \* Yutao Zhang, Bing Bai and Wei-Hong Zhu 

**The real-time monitoring of nitric oxide (NO) at the subcellular level is still a great challenge. To attain this goal, we developed a fast and selective near-infrared (NIR) fluorescent probe for the targeted tracing of endogenous NO. This probe possesses vital features for the real-time detection of intracellular NO including a significant turn-on NIR response, high specificity, and a fast response by a controlled photoinduced electron transfer (PET) process, which is applicable to the real-time monitoring of endogenous NO in mitochondria.**

Nitric oxide (NO), as a pivotal signalling molecule, is involved in diverse physiological and pathological processes.<sup>1–3</sup> Owing to its free radical nature with high reactivity, NO is generally quickly consumed by endogenous reactions in subcellular compartments.<sup>4</sup> Meanwhile, mitochondrial NO, which is mainly generated by inducible NO synthase (iNOS) enzymes in the subcellular organelles, plays a crucial role in regulating cell functions.<sup>5,6</sup> However, the role of mitochondrial NO in chemical biology is still not well established. The main obstacles are that endogenous NO is not only released at very low levels but also easily diffused and simultaneously consumed by thiol-containing biomolecules, which make it difficult to real-time *in situ* trace the local generation of NO in terms of organelles.<sup>7–10</sup> Hence, it is urgent to search for methods and tools that can real-time monitor NO distribution in mitochondria for better understanding of its origin, activities, and biological effects.

Owing to their high sensitivity and high spatial resolution, fluorescent probes afford great opportunities for the real-time mapping of the local distribution of NO in biological systems.<sup>11–18</sup> Accordingly, a number of NO fluorescent probes based on specific reactions with the *o*-phenylenediamino (OPD) moiety<sup>12,19,20</sup> have been designed to assess cellular NO-related events. Even though

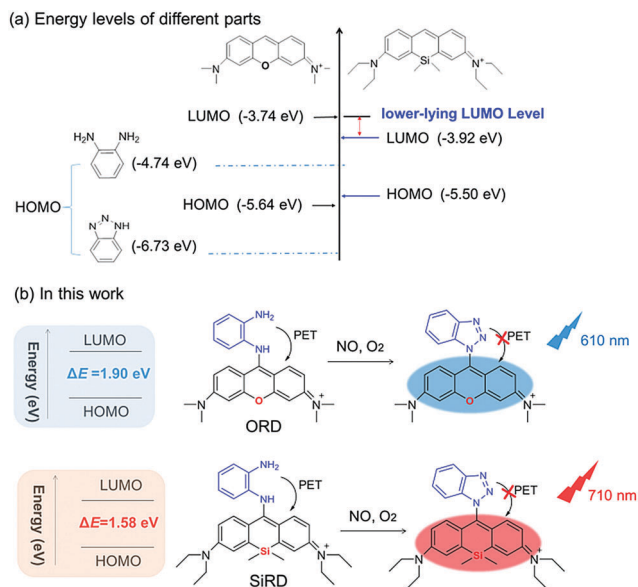
the well-developed OPD-based probes exhibit great potential for monitoring NO levels in living cells, most of them still suffer from the long-time reaction or short emission. So far, it has scarcely been reported on how to rationally design fast and selective near-infrared (NIR) fluorescent probes for the real-time and *in vivo* targeted monitoring of endogenous nitric oxide.<sup>21,22</sup>

As a general rule, an excellent NO fluorescent probe should meet these criteria of a rapid response, an NIR emission wavelength, and an organelle-targeting ability. As a significant work, Guo *et al.* reported a dual-channel OPD-based fluorescent probe for NO imaging.<sup>23</sup> Notably, the high specificity of this probe with NO could be attributed to the resulting unique triazole unit, unlike others. However, the slow reaction speed (~30 min) and short emission of this probe could prevent it *in vivo* real-time tracing NO.<sup>23</sup> The aforementioned concerns encouraged us to develop a novel fast and selective NIR fluorescent probe to real-time monitor mitochondria NO localization in living cells. To attain these goals, a promising silicon-substituted xanthene (SiR) NIR platform was directly conjugated with one of the amino groups in the OPD unit for the SiRD probe (Scheme 1) based on the following aspects: SiR fluorophores featuring excellent NIR spectral properties;<sup>24–27</sup> high specificity for NO;<sup>23</sup> and fast responses from the controlled photoinduced electron transfer (PET) process between SiR and OPD units.<sup>28</sup>

As illustrated in Scheme 1, the OPD moiety has a sufficient HOMO energy level to quench fluorescence by the PET process from the OPD unit to xanthene or silicon-substituted xanthene fluorophores. The replacement of oxygen by silicon for SiRD simultaneously affects both the HOMO and LUMO energy levels.<sup>26,27</sup> In particular, the obvious decrease in the LUMO level from  $-3.74$  to  $-3.92$  eV in SiRD indicates that it should be more suitable for the PET process with turn-on fluorescence switching. This lower-lying LUMO level could also increase the reaction rate of SiRD with NO.<sup>21</sup> Concurrently, the smaller energy band gap of SiRD could make a large red shift. Moreover, the positive charge of SiRD is expected to be cell-permeant and readily sequestered for the targeted mapping of mitochondria NO.<sup>23</sup> Thus, we predicted that SiRD will not only prolong the emission

Key Laboratory for Advanced Materials and Institute of Fine Chemicals, Shanghai Key Laboratory of Functional Materials Chemistry, School of Chemistry and Molecular Engineering, East China University of Science & Technology, Shanghai 200237, China. E-mail: guozq@ecust.edu.cn

† Electronic supplementary information (ESI) available. See DOI: 10.1039/c7cc05971j



**Scheme 1** (a) Energy levels of the OPD moiety and substituted fluoro-phores. (b) The design structures and proposed sensing mechanisms of ORD and SiRD with NO. Note: the smaller energy band gap of SiRD could make a large red shift and achieve long NIR emission.

into the NIR region, but also greatly enhance the reaction rate with NO.

To verify the aforementioned concerns, the photophysical properties of SiRD and ORD toward NO were investigated in HEPES buffer solution (50 mM, pH = 7.4, H<sub>2</sub>O : CH<sub>3</sub>CN = 7 : 3) at room temperature. As shown in Fig. 1, ORD and SiRD initially show main absorption peaks at 450 and 515 nm, respectively, but they are both non-fluorescent ( $\Phi_{\text{ORD}} = 0.0003$  and  $\Phi_{\text{SiRD}} = 0.0006$ ) due to an efficient PET mechanism. With the addition of 100 equiv. of DEA-NONOate, the initial absorption peak of SiRD sharply

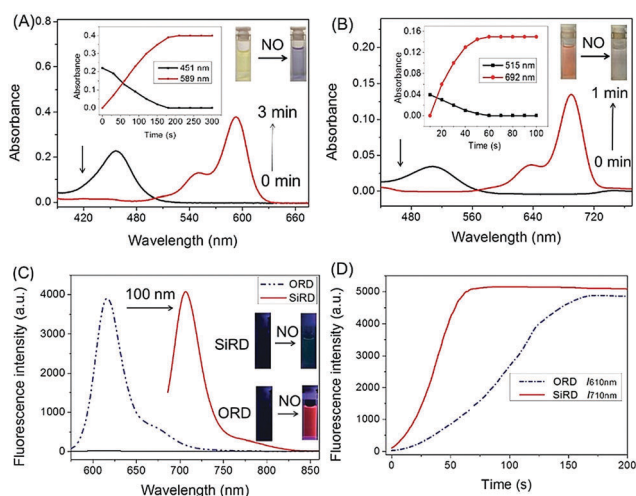


**Fig. 1** Spectral properties of ORD (5  $\mu\text{M}$ ) and SiRD (5  $\mu\text{M}$ ) in the presence of 100 equiv. of DEA-NONOate. Absorption spectra of (A) ORD and (B) SiRD. (C) Emission spectra of SiRD ( $\lambda_{\text{ex}} = 680 \text{ nm}$ ) and ORD ( $\lambda_{\text{ex}} = 570 \text{ nm}$ ). (D) Time-dependent emission spectra. Conditions: HEPES buffer (50 mM, pH = 7.4, H<sub>2</sub>O : CH<sub>3</sub>CN = 7 : 3).

decreased, as shown in Fig. 1B, while a new peak at 690 nm simultaneously appeared with a colour change from red to colourless (inset in Fig. 1B). Notably, a remarkable fluorescence enhancement at 710 nm ( $\Phi = 0.31$ ) was observed as a result of the blocking of the PET process (Fig. 1C). Based on the well-established reaction mechanism,<sup>23</sup> the spectral change could be ascribed to the resulting benzotriazole moiety, which was also supported by an HRMS experiment (Fig. S1 in the ESI<sup>†</sup>). Similar results were also observed for ORD in the presence of DEA-NONOate ( $\Phi = 0.25$ ) in the absorption and emission spectra in Fig. 1. In contrast, the turn-on fluorescence response of SiRD with NO falls into the NIR region, which is about 110 nm longer than that of ORD, especially preferable for *in vivo* bioimaging. In particular, it took only within 60 s for SiRD with NO reaching a reaction plateau but nearly 3 times longer for ORD with NO (Fig. 1D). Thus, the faster reaction and longer emission of SiRD towards NO are very favourable for the real-time detection of NO in living systems. Moreover, the probe is treated with NO under various concentrations (0 to 10  $\mu\text{M}$ ) to evaluate the sensitivity of SiRD to NO under simulated physiological conditions (Fig. S2, ESI<sup>†</sup>). The fluorescence intensity at 710 nm was linearly proportional to the NO concentration in the given range, indicating the suitability of SiRD for the quantitative and qualitative detection of NO potentially (Fig. S2, ESI<sup>†</sup>).

Then, the selectivity of SiRD toward NO over other possible interfering biologically relevant species, which include various biothiols (GSH, Cys, Hcy, Thr, Leu, Glu, Pro, Trp, Asa, Arg), reactive oxygen species (H<sub>2</sub>O<sub>2</sub>, HClO) and reactive nitrogen species (NO<sub>2</sub><sup>-</sup>, ONOO<sup>-</sup>), and ascorbic acid (AA), was investigated (Fig. 2). There are negligible fluorescence responses of the SiRD probe toward these relevant species. In contrast, only the SiRD probe with NO displayed an obvious turn-on NIR fluorescence at 710 nm, indicating its high selectivity towards NO. This could be attributed to the unique triazole unit resulting from the amino-protected OPD unit with NO (Fig. S1, ESI<sup>†</sup>). To further explore its practical applications, the effects of pH on SiRD in the absence and presence of NO were also studied, Fig. S3 (ESI<sup>†</sup>). The results indicated that both the probe itself and the reaction product were insensitive to pH in the 6.0–8.5 range. These properties ensure the reliability of using the SiRD probe to trace NO in physiological environments.

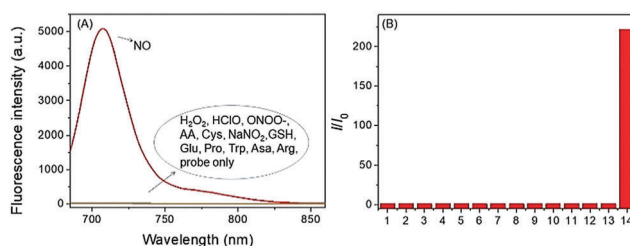


**Fig. 2** (A) Emission spectra of SiRD (5  $\mu\text{M}$ ) for NO over various species (100 equiv.) in HEPES buffer (50 mM, pH = 7.4, H<sub>2</sub>O : CH<sub>3</sub>CN = 7 : 3). (B) Fluorescence intensity changes at 710 nm: (1) probe only (5  $\mu\text{M}$ ), (2) H<sub>2</sub>O<sub>2</sub>, (3) HClO, (4) ONOO<sup>-</sup>, (5) AA, (6) Cys, (7) NaNO<sub>2</sub>, (8) GSH, (9) Glu, (10) Pro, (11) Trp, (12) Asa, (13) Arg, and (14) DEA-NONOate.  $\lambda_{\text{ex}} = 680 \text{ nm}$ .

All these aforementioned investigations confirmed that SiRD has a good ability to detect NO in aqueous solution. Notably, the resulting benzotriazole unit from probes with NO was previously reported to be a leaving group in S-acylation reactions.<sup>23</sup> In fact, some reported rhodamine derivatives acted as electrophiles when a nucleophile (for example, thiolate) is conjugated close to the xantheno ring of rhodamine, resulting in an intramolecular substitution reaction.<sup>29</sup> Thus, in our case, we also carefully studied the fluorescence response of SiRD toward NO in the presence of abundant cellular biothiols such as Cys and GSH. We envisioned that this intramolecular displacement reaction by biothiols could alter the degree of conjugation with the SiRD fluorophores, which brings about a change in fluorescence emission. With the titration of Cys (500  $\mu\text{M}$ ) in a pretreated solution of SiRD and DEA-NONOate, a new absorbance centred at 480 nm was observed, along with obvious colour changes. Correspondingly, new emission at 620 nm was also found when excited at 480 nm (Fig. S4, ESI<sup>†</sup>). The same results were also observed for SiRD upon treatment with Cys and the subsequent addition of DEA-NONOate (Fig. S5, ESI<sup>†</sup>). The HRMS results confirmed our proposed mechanism, wherein the intramolecular displacement product of sulfur with the amino group of Cys was clearly observed (Fig. S6, ESI<sup>†</sup>).<sup>30–33</sup> However, with the addition of GSH to the pretreated solution of SiRD and DEA-NONOate, only subtle spectral changes were observed (Fig. S8, ESI<sup>†</sup>). It could be because the bulky tripeptide of GSH would hinder the intramolecular displacement reaction. So, these results implied that intracellular NO could be detected using the SiRD probe from two different fluorescent channel signals assisted by intracellular Cys. Also, the titration of Cys (0 to 400  $\mu\text{M}$ ) with the pretreated solution of SiRD with NO was also investigated (Fig. S7, ESI<sup>†</sup>). The fluorescence intensity at 610 nm was linearly proportional to the Cys concentrations in the given range, indicating the potential quantitative and qualitative detection of Cys.

To examine the usability of the SiRD probe for the subcellular labeling and monitoring of NO in living cells, we first evaluated the cytotoxicity by using HeLa cell lines. An MTT assay revealed that 80% of the HeLa cells survived even after incubation with SiRD (10.0  $\mu\text{M}$ ) for 12 h (Fig. S9, ESI<sup>†</sup>). Subsequently, we evaluated the capability of SiRD to real-time monitor NO in living cells. When the HeLa cells were incubated with SiRD (2  $\mu\text{M}$ ), almost no fluorescence was found in both the red ( $\lambda_{\text{ex}} = 488 \text{ nm}$ ,  $\lambda_{\text{em}} = 550\text{--}670 \text{ nm}$ ) (Fig. 3B) and purple ( $\lambda_{\text{ex}} = 630 \text{ nm}$ ,  $\lambda_{\text{em}} = 690\text{--}740 \text{ nm}$ ) channels (Fig. 3C). After that, the pretreated cells were incubated with a good inhibitor of intracellular biothiols (NEM, 200  $\mu\text{M}$ ) for 30 min; obviously strong NIR emission in the purple channel was immediately observed in the presence of DEA-NONOate (Fig. 3G), while there was no fluorescence in the red channel (Fig. 3F). These results clearly indicate that the SiRD probe meets the requirements for the real-time monitoring of exogenous NO from nitric oxide precursors in living cells.

Moreover, in order to evaluate the effect of intracellular biothiols, cysteine (200  $\mu\text{M}$ ) was added to the cells stained with the SiRD probe in the presence of DEA-NONOate, only strong fluorescence signals in the red channel (Fig. 3J) were observed, verifying our proposed detection mechanism that the SiRD probe could sense intracellular NO assisted by intracellular

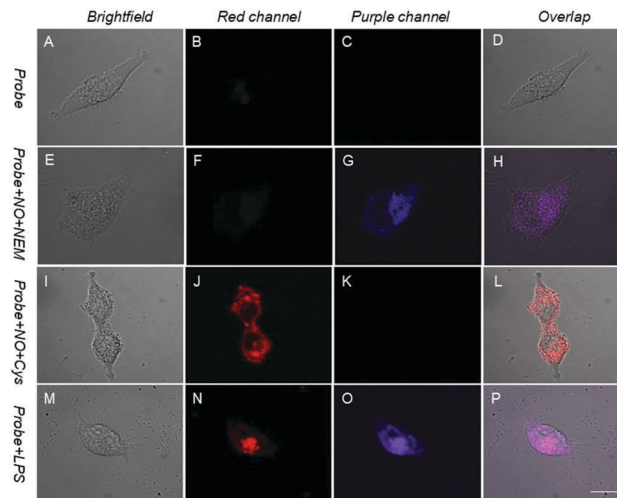
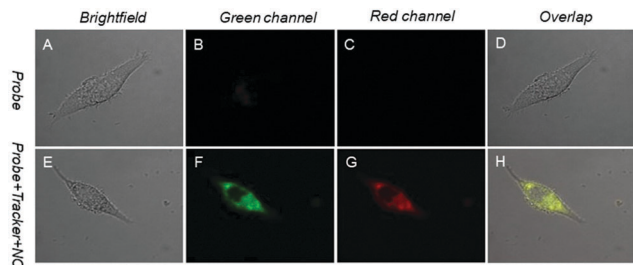


Fig. 3 Fluorescence imaging of exogenous and endogenous NO with the SiRD probe (2  $\mu\text{M}$ ) in HeLa cells. (A–D) Images of cells pre-incubated with the SiRD probe for 30 min; and (E–H) then incubated with a good inhibitor of intracellular biothiols (NEM, 200  $\mu\text{M}$ ) in the presence of DEA-NONOate (200  $\mu\text{M}$ ) for 30 min. (I–L) fluorescence images of cells stained with the SiRD probe that were incubated with DEA-NONOate (200  $\mu\text{M}$ ) and Cys (200  $\mu\text{M}$ ) for 30 min. (M–P) fluorescence images of cells stained with the SiRD probe that were incubated with the NO stimulant LPS (20  $\mu\text{g mL}^{-1}$ ) for 12 h. Fluorescence signals were collected at 550–670 nm for the red channel ( $\lambda_{\text{ex}} = 488 \text{ nm}$ ), and collected at 690–740 nm for the purple channel ( $\lambda_{\text{ex}} = 638 \text{ nm}$ ). The scale bar represents 10  $\mu\text{m}$ .

Cys (Fig. S10, ESI<sup>†</sup>). We further attempted to apply the SiRD probe to monitor the locally generated endogenous NO in living cells. Inducible endogenous NO in HeLa cells could be activated by lipopolysaccharides (LPS).<sup>22,34</sup> As shown in Fig. 3N and O, after the incubation of LPS (20  $\mu\text{g mL}^{-1}$ ) for 12 h, the cells were treated with the SiRD probe for 30 min, displaying desired strong fluorescence signals in both the red and purple channels because of the existence of endogenous Cys and NO. Clearly, it was indicated that the SiRD probe shows excellent ability to real-time image endogenous NO.

Meanwhile, the SiRD probe possessing a positive charge exhibits a significant ability to target mitochondria.<sup>35,36</sup> To confirm that the SiRD probe was a mitochondria-targetable probe for NO, co-localization experiments were performed by co-staining HeLa cells with the SiRD probe and MitoTracker Green FM (a commercial mitochondria tracker). Initially, HeLa cells with the SiRD probe did not exhibit fluorescence in the red channel (Fig. 4C); after these cells were further incubated in the presence of 200 equiv. of DEA-NONOate for 30 min, they displayed strong fluorescence in discrete subcellular locations (Fig. 4G). The yellow merged image (Fig. 4H, high Pearson's colocalization coefficient 0.98) indicates that the staining of SiRD fits well with that of mitochondrial tracker Green FM (Fig. 4F). These results provide solid evidence for the SiRD probe's mitochondrial specificity (Fig. S11, ESI<sup>†</sup>).

In summary, we presented a fast and selective near-infrared (NIR) fluorescent probe for the real-time and *in vivo* targeted monitoring of endogenous nitric oxide. It is found that the replacement of oxygen with silicon atoms can efficiently narrow



**Fig. 4** SiRD colocalizes to the mitochondria in HeLa cells. (A–D) HeLa cell was stained with SiRD (2  $\mu$ M) for 30 min. (E–H) Fluorescence images of HeLa cells with the probe (2  $\mu$ M) with DEA-NONOate (200  $\mu$ M) for 30 min, and then costained with Mito Tracker Green FM (0.2  $\mu$ M) for 30 min. Fluorescence signals were collected at 550–670 nm for the red channel ( $\lambda_{\text{ex}} = 488$  nm) and collected at 500–530 nm for the green channel ( $\lambda_{\text{ex}} = 488$  nm).

the bandgap between the HOMO and LUMO and extend the emission wavelength. To prolong the emission into the NIR region and enhance the reaction speed with NO, the SiRD probe was carefully designed by directly conjugating a silicon-substituted xanthene (SiR) NIR platform with one of the amino groups in OPD units. In our strategy, the controlled photo-induced electron transfer (PET) process was realized between SiR and OPD units. It was demonstrated that the SiRD probe possesses significant features for the selective detection of NO, including a turn-on NIR response at 710 nm, a fast response within 1 min, and specific localization in mitochondria. Cell experiments also confirmed this probe's applicability to detection of endogenous and exogenous NO in the mitochondria of living cells. We anticipate that this excellent NIR probe could provide more opportunities to gain insight into the regulation of the biological effects of NO.

This work was supported by the National Key Research and Development Program (No. 2017YFC0906902), Excellent Young Scholars (21622602), Distinguished Young Scholars (21325625), the Key Project (21636002), the NSFC/China, the Oriental Scholarship, the Scientific Committee of Shanghai (14ZR1409700 and 15XD1501400), the Fok Ying Tong Education Foundation (142014), and the Fundamental Research Funds for the Central Universities.

## Conflicts of interest

There are no conflicts to declare.

## Notes and references

- 1 C. Bogdan, *Nat. Immunol.*, 2001, **2**, 907.
- 2 S. H. Snyder, *Science*, 1992, **257**, 494.

- 3 D. Fukumura, S. Kashiwagi and R. K. Jain, *Nat. Rev. Cancer*, 2006, **6**, 521.
- 4 A. G. Tennyson and S. J. Lippard, *Chem. Biol.*, 2011, **18**, 1211.
- 5 M. A. Marletta, *Cell*, 1994, **78**, 927.
- 6 U. Forstermann, I. Gath, P. Schwarz, E. I. Closs and H. Kleinert, *Biochem. Pharmacol.*, 1995, **50**, 1321.
- 7 H. Yu, X. Zhang, Y. Xiao, W. Zou, L. Wang and L. Jin, *Anal. Chem.*, 2013, **85**, 7076.
- 8 H. Yu, Y. Xiao and L. Jin, *J. Am. Chem. Soc.*, 2012, **134**, 17486.
- 9 B. Wang, S. Yu, X. Chai, T. Li, Q. Wu and T. Wang, *Chem. – Eur. J.*, 2016, **22**, 5649.
- 10 C. Wang, X. Song, Z. Han, X. Li, Y. Xu and Y. Xiao, *ACS Chem. Biol.*, 2016, **11**, 2033.
- 11 X. Zhou, S. Lee, Z. Xu and J. Yoon, *Chem. Rev.*, 2015, **115**, 7944.
- 12 N. Gupta, S. Imam Reja, V. Bhalla, M. Gupta, G. Kaur and M. Kumar, *Chem. – Asian J.*, 2016, **11**, 1020.
- 13 X. Chen, F. Wang, J. Y. Hyun, T. Wei, J. Qiang, X. Ren, I. Shin and J. Yoon, *Chem. Soc. Rev.*, 2016, **45**, 2976.
- 14 X. Zhou, Y. Zeng, C. Liyan, X. Wu and J. Yoon, *Angew. Chem., Int. Ed.*, 2016, **55**, 4729.
- 15 J. Miao, Y. Huo, X. Lv, Z. Li, H. Cao, H. Shi, Y. Shi and W. Guo, *Biomaterials*, 2016, **78**, 11.
- 16 X. Sun, Y. Xu, W. Zhu, C. He, L. Xu, Y. Yang and X. Qian, *Anal. Methods*, 2012, **4**, 919.
- 17 S. Ma, D. C. Fang, B. Ning, M. Li, L. He and B. Gong, *Chem. Commun.*, 2014, **50**, 6475.
- 18 Z. Mao, H. Jiang, Z. Li, C. Zhong, W. Zhang and Z. Liu, *Chem. Sci.*, 2017, **8**, 4533–4538.
- 19 H. W. Yao, X. Y. Zhu, X. F. Guo and H. Wang, *Anal. Chem.*, 2016, **88**, 9014–9021.
- 20 Y. Hu, L. Chen, H. Jung, Y. Zeng, S. Lee, K. M. K. Swamy, X. Zhou, M. H. Kim and J. Yoon, *ACS Appl. Mater. Interfaces*, 2016, **8**, 22246.
- 21 Z. Guo, S. Park, J. Yoon and I. Shin, *Chem. Soc. Rev.*, 2014, **43**, 16–29.
- 22 Z. Mao, W. Feng, Z. Li, L. Zeng, W. Lv and Z. Liu, *Chem. Sci.*, 2016, **7**, 5230–5235.
- 23 Y. Q. Sun, J. Liu, H. Zhang, Y. Huo, X. Lv, Y. Shi and W. Guo, *J. Am. Chem. Soc.*, 2014, **136**, 12520–12523.
- 24 Y. Q. Sun, J. Liu, X. Lv, Y. Liu, Y. Zhao and W. Guo, *Angew. Chem., Int. Ed.*, 2012, **51**, 7634.
- 25 Y. Gabe, Y. Urano, K. Kikuchi, H. Kojima and T. Nagano, *J. Am. Chem. Soc.*, 2004, **126**, 3357.
- 26 M. Fu, Y. Xiao, X. Qian, D. Zhao and Y. Xu, *Chem. Commun.*, 2008, 1780.
- 27 Y. Kushida, T. Nagano and K. Hanaoka, *Analyst*, 2015, **140**, 685–695.
- 28 K. Tanaka, T. Miura, N. Umezawa, Y. Urano, K. Kikuchi, T. Higuchi and T. Nagano, *J. Am. Chem. Soc.*, 2001, **123**, 2530.
- 29 K. Umezawa, M. Yoshida, M. Kamiya, T. Yamasoba and Y. Urano, *Nat. Chem.*, 2017, **9**, 279–286.
- 30 L.-Y. Niu, Y.-S. Guan, Y.-Z. Chen, L.-Z. Wu, C.-H. Tung and Q.-Z. Yang, *Chem. Commun.*, 2013, **49**, 1294.
- 31 L.-Y. Niu, Y.-S. Guan, Y.-Z. Chen, L.-Z. Wu, C.-H. Tung and Q.-Z. Yang, *J. Am. Chem. Soc.*, 2012, **134**, 18928.
- 32 F. Wang, P. Y. Zhu, L. Zhou, L. Pan, Z. Cui, Q. Fei, S. Luo, D. Pan, Q. Huang, C. Zhao, H. Tian and C. H. Fan, *Angew. Chem., Int. Ed.*, 2015, **54**, 7349.
- 33 Y. Yue, F. Huo, P. Ning, Y. Zhang, J. Chao, X. Meng and C. Yin, *J. Am. Chem. Soc.*, 2017, **139**, 3181.
- 34 H. Zhang, J. Liu, Y. Q. Sun, Y. Huo, Y. Li, W. Liu, X. Wu, N. Zhu, Y. Shi and W. Guo, *Chem. Commun.*, 2015, **51**, 2721–2724.
- 35 C. Han, H. Yang, M. Chen, Q. Su, W. Feng and F. Li, *ACS Appl. Mater. Interfaces*, 2015, **7**, 27968.
- 36 D. Cheng, Y. Pan, L. Wang, Z. Zeng, L. Yuan, X. Zhang and Y. T. Chang, *J. Am. Chem. Soc.*, 2017, **139**, 285–292.